Z-Tagging Mini DIRC

C.E. Hyde[*†3], Wenliang Li[*1,2], V. Baturin[3], Jan Bernauer[1,2], Ross Corliss[1,2], Ethan Cline[1,2,8], Jaydeep Datta[1,2], Abhay Deshpande[1,2], Roman Dzhygadlo[5], Thomas K. Hemmick[1,2], Yordanka Ilieva[6], Grzegorz Kalicy[4], Brynna Moran[1,2], Charles-Joseph Naim[1,2], Nathan Shankman[1,2], Evgeny Shulga[1,2], Pawel Nadel-Turonski[1,2], Barak Schmookler[7], Jochen Schwiening[5], Carsten Schwarz[5], and Nilanga Wickramaarachchi[4]

[1]Stony Brook University, Stony Brook, NY 11794, USA
[2]Center for Frontiers in Nuclear Science, Stony Brook University, Stony Brook, NY 11794, USA
[3]Old Dominion University, Norfolk VA 23529, USA
[4]Catholic University of America, Washington D.C. 20064, USA
[5]GSI Helmholtz Centre for Heavy Ion Research, Darmstadt, Germany
[6]University of South Carolina, Columbia, South Carolina 29208, USA
[7]University of California Riverside, Riverside, CA 92521, USA
[8]Massachusetts Institute of Technology, Cambridge, MA 02139, USA

July 14, 2023

Abstract

We propose an R&D program for a fused silica Cherenkov detector at the high dispersion downstream ion focus of the Interaction Region (IR) of a proposed second EIC detector. The goal of the detector is to resolve the discrete charge of nuclear fragments produced in eA collisions. This capability would greatly enhance the ability to separate coherent nuclear processes from incoherent channels. Tagging the charge of nuclear fragments in coincidence with detection of decay photons would enable a unique program of rare isotope spectroscopy with nuclear half-lives as short as ~ 1 nsec. We will simulate the Cherenkov light production of primary ions, secondary δ-rays and other background sources. This program will establish whether such a detector can achieve the performance seen in preliminary studies, and meet the challenges of measuring light pulses with a 10,000:1 dynamic range with Poisson-statistics precision.

[*]Co-spokesperson
[†]Contact person, chyde@odu.edu

Contents

1 Introduction & Motivation

Recent studies have illustrated the potential of the Electron Ion Collider (EIC) to detect short-lived rare isotopes produced in eA collisions [1]. The daughter isotopes are generally produced as either evaporation residues (ER) or fission fragments (FF). In either case, the daughter isotopes have a magnetic rigidity close to the original beam ion, but slightly different due to the variable charge-to-mass ratios of the daughter ions. In addition, evaporation residues are created with only minimal transverse momentum relative to the ion beam axis. Even fission fragments receive a transverse kick less than twice the RMS transverse momentum of the ion beam at the Interaction Point (IP). The potential for resolving ERs from the ion beam is illustrated in Fig. 1, both for the Project Detector Interaction Region 6 (IR6) ion optics and for proposed IR8 ion optics. The Interaction Region 8 (IR8) proposed for a

second detector includes a high dispersion second focus approximately 48 m downstream of the interaction point (IP). The physics potential of rare isotope tagging at a second IR was highlighted in the DPAP report [2].

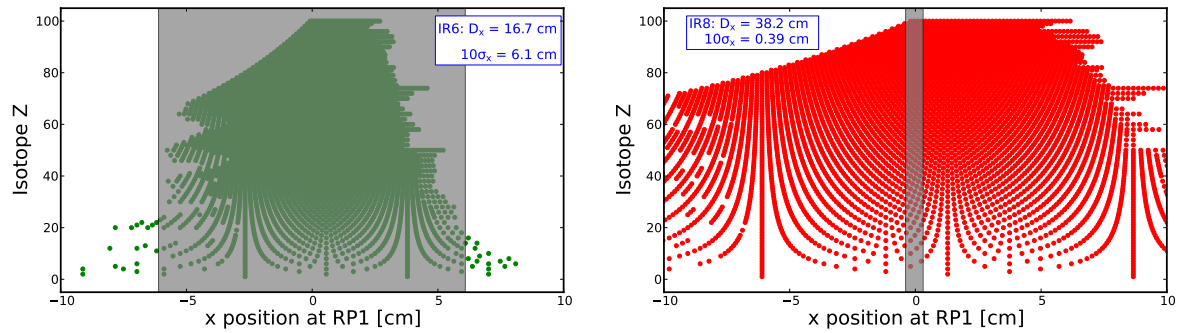

Figure 1: Isotope z vs. hit position in the best Roman pot in IR6 (left) and IR8 (right), respectively [1]. The gray box on each plot shows the 10σ beam size which prevents detection. This exclusion is much smaller in IR8 due to the 2^{nd} focus. The larger horizontal spacing in IR8 is due to a larger dispersion. The isotopes shown assume a ^{238}U beam, but are representative for all heavy ions. The exceptional ability of IR8 to detect fragments with magnetic rigidities very close to that of the beam is also indicative of the acceptance for recoil protons and nuclei that emerge from exclusive reactions with a low p_T with respect to the beam.

The Zero Degree Calorimeter (ZDC) and the gap inside of the first downstream dipole–B0 (but outside the beam pipe) can be instrumented with high resolution electromagnetic calorimetry to detect boosted decay photons in coincidence with the tagged ion at the second focus. In this way the excitation spectra of rare isotopes can be measured, particularly for short lived isotopes that are not accessible at FRIB and other facilities.

Tagging ion beam fragments is also essential for resolving coherent deep virtual exclusive scattering processes (*e.g.* $e + Pb \rightarrow e' + J/\Psi + Pb$) from incoherent scattering in which one or more nucleons are emitted.

In this proposal, we describe an R&D program for a small detector capable of identifying the nuclear charge z of ion fragments detected in the Roman Pots (RP) at the second focus. This mini Detector of Internally Reflected Cherenkov light (mini-DIRC) would consist of a thin quartz radiator coupled to a light collection volume and a high resolution photo-sensor. The z-dependent signal is the event-by-event absolute intensity of the Cherenkov light pulse. The mini-DIRC design goal is to measure the light pulse from a heavy projectile with relative stability $\leq 1\%$ for $z = 90$.

2 Cherenkov Signal

In a medium of index of refraction $n(\lambda)$, the Cherenkov photon emission per unit length dX along the particle track and per unit wavelength for a particle of velocity $\beta > 1/n(\lambda)$ is [3]:

$$\frac{dn_\gamma(\lambda)}{dXd\lambda} = z^2 \frac{2\pi\alpha}{\lambda^2}\left[1 - \frac{1}{\beta^2 n^2(\lambda)}\right] \tag{1}$$

2.1 Fused Silica

The index of refraction of fused silica, from the near UV to near IR is plotted in Fig. 2. This is also described by the dispersion equation [4]:

$$n^2(\lambda) - 1 = \frac{0.6962}{1 - [(68.40\text{ nm})/\lambda]^2} + \frac{0.4079}{1 - [(116.2\text{ nm})/\lambda]^2} + \frac{0.8975}{1 - [(9.896\,\mu\text{m})/\lambda]^2} \tag{2}$$

Given a photo-sensor of quantum efficiency $\epsilon(\lambda)$ (which also depends on photon arrival position on the sensor) and a light collection acceptance $a(\lambda)$ (which is also a transfer function from particle position to position on sensor), the projected number of detected photo-electrons is

$$N_{p.e.}(z) = \Delta X \int d\lambda \frac{dn_\gamma(\lambda)}{dXd\lambda}\epsilon(\lambda)a(\lambda) \tag{3}$$

Based on the BABAR and PANDA DIRC experience, we anticipate a detection threshold of 280 nm. Integrating over the quantum efficiency of a Hamamatsu MCP-PMT R10754-07-M16 [5] and applying a 50% collection efficiency implies a total signal of $2{\cdot}10^5$ photo-electrons for a relativistic ion of $z = 90$ incident on a 0.6 cm thick SiO_2 bar. The collection efficiency, quantum efficiency and spectral range are all subject to revision and optmization. In any case, it is clear that the raw photo-emission is more than sufficient to achieve $\delta z/z \leq 1\%$ at $z = 90$. On the other hand, a successful detector must control any event-by-event fluctuations in light collection, quantum efficiency, gain non-linearity and noise (both electronic and particle background.

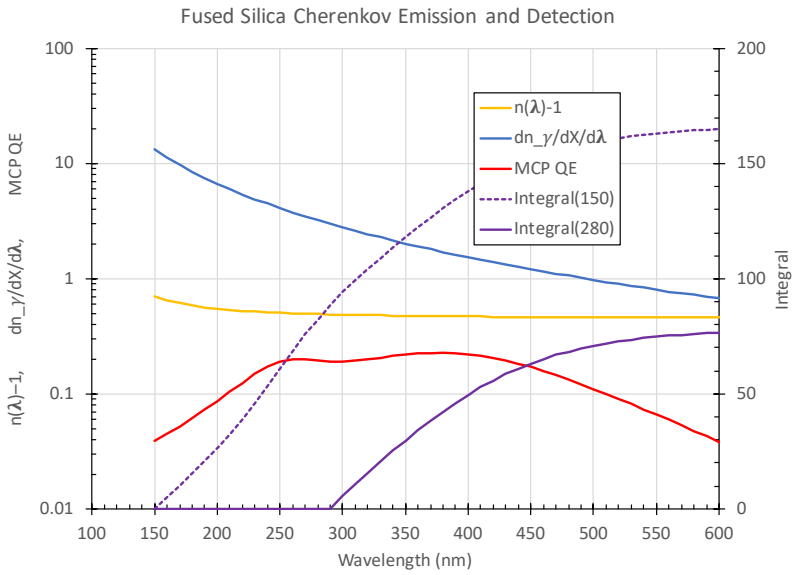

Figure 2: Index of refraction of SiO_2 (Yellow curve: $n(\lambda) - 1$) [4]. Cherenkov light yield (blue curve, projectile charge $z = 1$), units: 1/nm/cm. Quantum efficiency of Hamamatsu MCP PMT (Red curve) [5]. Integral of Eq. 3 (purple curves, right vertical axis), with charge $z = 1$, $\Delta X = 1$ cm and $a(\lambda) = 1$. Light collection and detection thresholds are $\lambda = 150$ and 280 nm for the dashed and solid curves, respectively.

2.2 Ray Trace Simulations

We have conducted an initial simulation of a $z = 90$ ion passing through a 1 cm thick SiO_2 radiator coupled to an expansion volume. This is shown in Fig. 3. Qualitatively, the photosensor surface is uniformly illuminated. The comparison of the photon yield for $z = 90$ and $z = 91$ ions in Fig. 4 shows excellent separation.

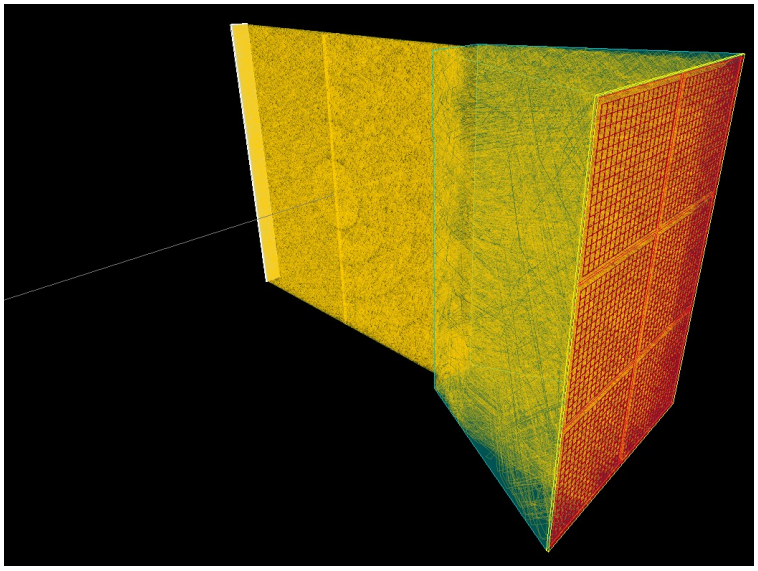

Figure 3: Ray trace of 10% of Cherenkov photons from a relativistic $z = 90$ ion, passing through a 1 cm thick silica radiator. The light collection efficiency is 95%.

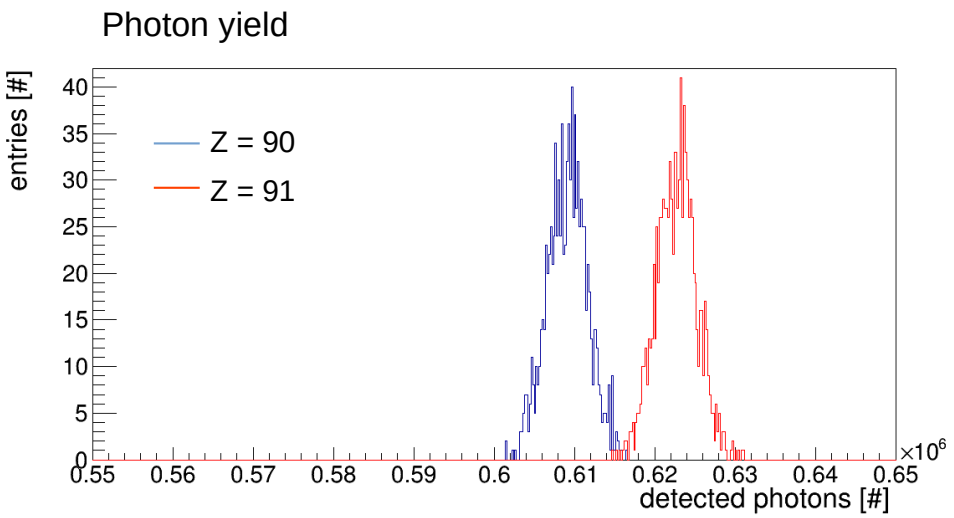

Figure 4: Comparison of the photon detection yield for $z = 90$ and $z = 91$ ions. The photo detection quantum efficiency is 30% for 280 nm to 400 nm. The statistical fluctuations correspond to only 10% of the Cherenkov yield, but the histogram is rescaled to the full yield.

2.3 Energetic δ-Rays

In addition to the direct Cherenkov light of the primary ion, there may be a significant (and fluctuating) signal from energetic secondaries (δ-rays) produced by passage of the primary ion through the quartz. The distribution of secondary electron of energy T_e, with $I \ll T_e \ll W_{\rm Max}$, is [3]:

$$\begin{aligned}
\frac{d^2N_\delta}{dX\,dT} &\approx \frac{z^2 K\rho}{2\beta^2}\left\langle\frac{z}{A}\right\rangle\frac{1}{T_e^2}\\
K &= 0.307\frac{\text{MeV cm}^2}{\text{mole}}\\
W_{\rm Max} &= \frac{2m_e\beta^2\gamma^2}{1+2\gamma m_e M_z+(m_e/M_z)^2}\\
I(\text{SiO}_2) &= 139\text{eV}, \qquad \rho(\text{SiO}_2) = 2.20\ \text{g/cm}^3.
\end{aligned} \tag{4}$$

Note that δ-ray production also scales as the projectile charge squared (z^2). The δ-ray threshold for visible Cherenkov radiation in fused silica is $T_e = T_{\rm Th} = 210$ KeV. The integrated flux of secondary electrons above Cherenkov threshold in SiO_2 is

$$\frac{dN}{dX} \approx z^2\,(0.013/\text{cm}) = \frac{106}{\text{cm}} \text{ for } z = 90. \tag{5}$$

With the same light collection assumptions described above, each of these secondaries with produce on average approximately 38 Cherenkov photo-electrons (Fig. 2), for a total yield

from an ion $z = 90$ of 4000 photo-electrons, which is just over 1% of the direct Cherenkov yield.

2.4 Gain Saturation Effects

We give here a semi-analytic estimate of gain saturation effects if SiPMs are chosen as the photo sensor. More detailed numerical simulations will be carried out if this project is funded.

Based on the previous analysis we assume $N_{pe} = 2.4 \cdot 10^5$ photo-electrons are produced by a $z = 90$ ion in a 30×30 mm^2 SiPM array. With 3×3 mm^2 readout pixels, each pixel contains 90,000 micropixels ($(10\,\mu\text{m})^2$ each) and the total number of micropixels in the full array is $N_{\mu P} = 9 \cdot 10^6$. The average occupancy per micropixel is then $\mu = N_{pe}/N_{\mu P} = 2.7\%$. Given a single photon pulse amplitude of S_0, The total signal is

$$S = N_{\mu P} S_0 \left(1 - e^{-\mu}\right) = N_{pe} S_0 \left(1 - e^{-\mu}\right)/\mu \qquad \Rightarrow 0.987 N_{pe} S_0 \quad \text{at } \mu = 2.7\% \tag{6}$$

With $N_{pe} = z^2 n_0$, the z-dependent gain saturation effect is

$$S(z) = z^2 n_0 S_0 \left(1 - e^{-\mu}\right)/\mu = N_{\mu P} S_0 \left(1 - e^{-z^2 n_0 / N_{\mu P}}\right) \tag{7}$$

To resolve ions $z \pm 1$, we require

$$\begin{aligned} \frac{1}{z} < \frac{1}{S(z)} \frac{dS}{dz} &= \frac{2\mu e^{-\mu}}{z\left(1 - e^{-\mu}\right)} \\ \left(1 + 2\mu\right) e^{-\mu} > 1 \qquad &\Rightarrow \quad \mu < 1.25 \end{aligned} \tag{8}$$

Thus the individual micro-pixel saturation does not seem to be a problem, even if larger (*e.g.* $(25\,\mu\text{m})^2$ micro pixels are used).

A second gain saturation question is whether the large amplitude pulses with reduce the gain by drawing too much charge from the bias capacitance. For the Hamamatsu S14160-3110PS MPPS, a single $(3\text{ mm})^2$ readout pixel has a capacitance of 530 pF. At a gain of $G = 2 \cdot 10^5$, a $z = 90$ ion will produce a single channel pulse

$$\begin{aligned} S_{\text{Channel}} &= (2.4 \cdot 10^3 \text{p.e.})(2 \cdot 10^5 e) \\ &= 77 \text{ pC} \end{aligned} \tag{9}$$

The gain varies as $dG/dV \approx 0.4 \cdot 10^5$ per Volt. This implies a gain shift of 0.3% between a $z = 90$ and $z = 89$ ion, whereas the signal difference is 2.2%.

In conclusion, a variety of semi-analytic tests support the idea that a thin quartz radiator can resolve the charge of incident ions with a resolution $\sigma(z) < 1$ across the chart of nuclides. We believe this concept warrants more comprehensive numerical simulation and possible prototype tests.

3 Background Studies

In eRD21 [6], we performed FLUKA simulations of backgrounds in the EIC detector from proton beam – residual gas interactions, and the physics ep collisions. Fig.5 illustrates the beam-gas generated backgrounds for IR6 (Project Detector). The FLUKA model includes all beam line elements within ± 50 m of the IP. For this project, we will adapt the model for IR8. This includes increasing the crossing angle at the IP from 25 to 35 mrad and switching the polarity of the first downstream ion dipole (B0). This moves the ZDC to the outside of the ion beam. Instead of the dipole at ~ 48 m, a dipole/quadrupole pair are introduced at 35-40 m. The full proposed IR8 ion optics, described in Table 1 and Fig. 3 produces a high dispersion focus 48 m downstream of the IP.

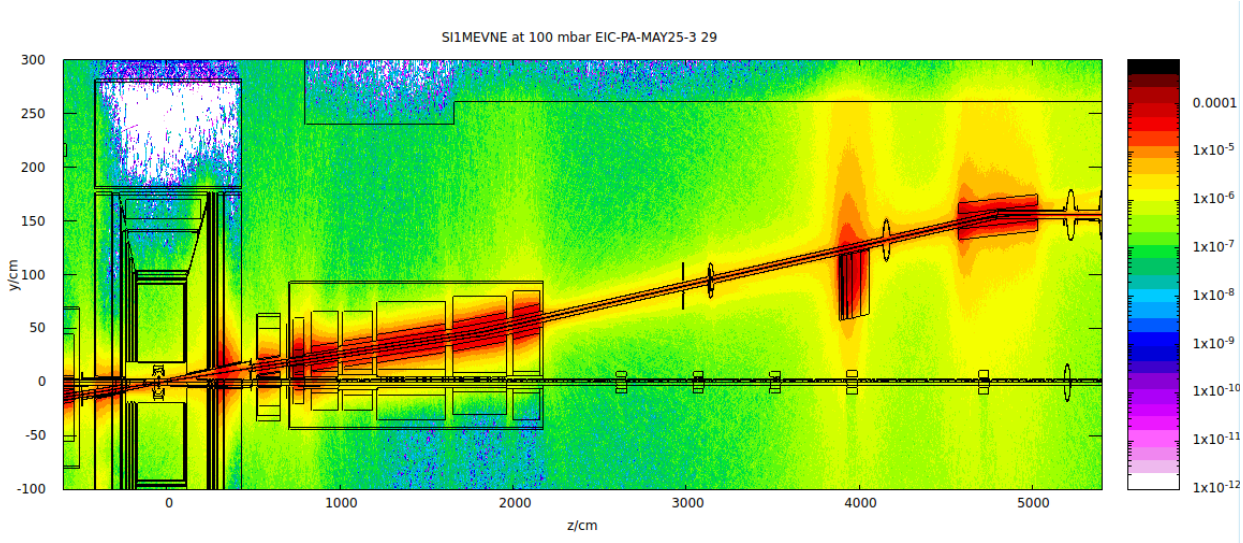

Figure 5: Neutron 1 MeV equivalent fluence in the ion downstream area (IP at -50 cm). Neutron fluence (color scale, neutrons/cm^2) is given per primary proton and at residual gas pressure $P_F = 100$ mbar. Horizontal scale: z coordinate opposite electron beam axis in cm. Vertical scale: horizontal coordinate (Y) in cm. The proton beam may be seen in this plot as a black line ("snake") following the two bending magnets. ZDC is at 40 m. Actual neutron fluence with 1 A protons and 10^{-9} mbar is obtained by multiplying color scale by $6.25 \cdot 10^7$/sec. With this scaling, maximal fluence in the ZDC is $2 \cdot 10^4$n/cm^2/s.

The primary purpose of new background studies will be to understand the charged particle backgrounds from heavy ion beams in the Roman Pot detectors. Aside from the physics processes of interest, we consider two sources of a random energetic heavy ions striking the MiniDIRC radiator. The first is diffractive dissociation of projectile ions by interactions with the residual gas in the beam pipe. The second is photo-excitation of the beam projectile ions in eA collisions at the IP. Our initial conclusions, described below, is that there is only a $\sim 0.1\%$ probability of background pile-up to a physics event in the Roman Pot detectors at the downstream focus.

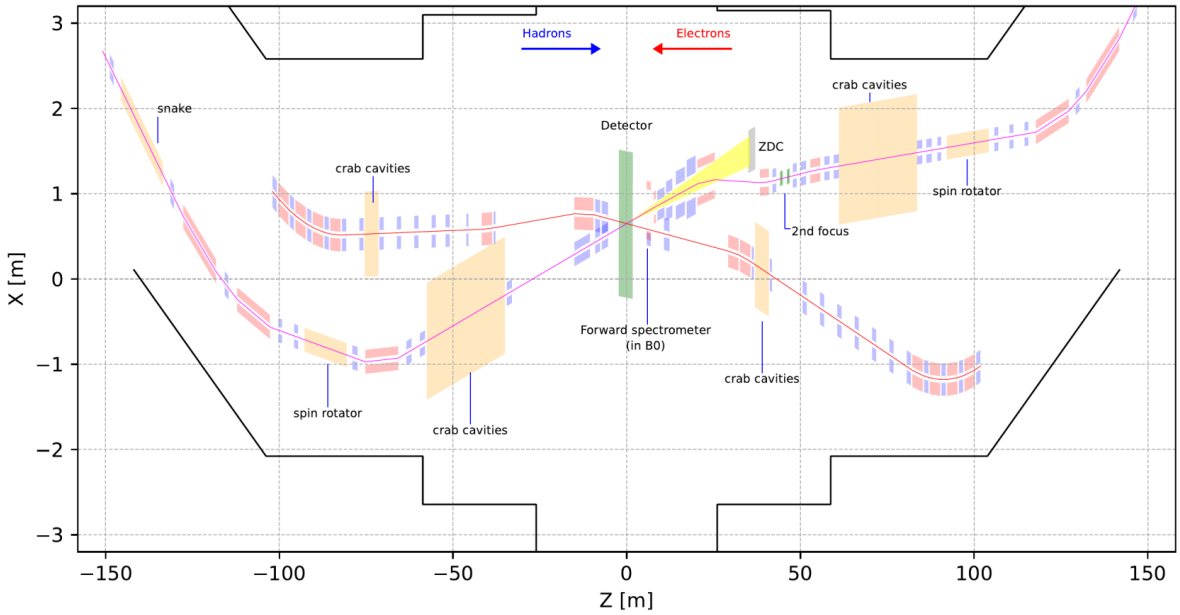

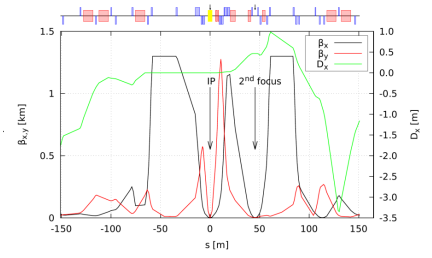

Parameters at the 2nd focus for different energies

Parameter	41 GeV	Value at 100 GeV	275 GeV	Units
β_x	0.85	0.8	0.5	m
D_x	0.48	0.48	0.47	m
ϵ_x	44	30	11.3	nm
σ_δ (10^{-4})	10.3	9.7	6.8	-
$1-x_L$ (10^{-3})	4.16	10.2	7	-

Figure 6: Interaction Region 8 (IR8) draft layout (top) and optics parameters (right) [7]. The rms fractional momentum spread of the ion beam is σ_δ. The longitudinal rigidity detection exclusion zone at 0° is given by $\pm|1-x_L|$. At 275 GeV, this is 0.7%. This is the gray zone in Fig. 1 (right). The downstream ion magnets are described in Table 1.

Table 1: IR8 Ion Downstream Beamline Elements. Coordinates $(x_0, 0, z_0)$ are the centers of the magnets. All distances are in m. Field is B_y(T) for Dipoles and $\partial B_y/\partial x$ (T/m) for Quadrupoles. Each magnet axis is rotated by $-\theta_y$ in the x-z plane.

Name	Type	Length	r_{In}	r_{Exit}	r_{Outer}	Field	x_0	z_0	θ_y (rad)
ionBXSP01	Dipole	1.2	0.245	0.245	0.345	4.587	0.212	6.096	0
ionQFFDS01A	Quad	2.0	0.061	0.061	0.144	−63.51	0.260	8.196	0.043
ionQFFDS01B	Quad	2.2	0.086	0.086	0.194	−45.38	0.347	10.794	0.042
ionQFFDS02A	Quad	2.6	0.112	0.112	0.258	34.18	0.483	14.192	0.023
ionQFFDS02B	Quad	2.4	0.125	0.125	0.312	31.14	0.574	17.190	0.037
ionBXDS01A	Dipole	4.80	0.190	0.190	0.29	4.443	0.738	21.288	0.031
ionBXDS01B	Dipole	3.60	0.1	0.1	0.2	−4.597	0.905	38.488	0.022
ionQDS01	Quad	1.5	0.1	0.1	0.2	2.527	0.983	41.537	0.029

3.1 Ion Beam Interactions with Residual Gas

The pp total cross sections were fit by Donnachie and Landshoff [8] to a simple Regge form:

$$\sigma_{pp}(s) = (21.70\,\mathrm{mb})s^{0.0808} + (56.08\,\mathrm{mb})s^{-0.4525} \tag{10}$$

For an incident heavy ion with momentum per nucleon 110 GeV/u, the equivalent pp or np CM energy in a collision with a residual gas proton is 13.76 GeV. Guzey and Strikman [9] calculated pA cross sections in a Glauber-Gribov formalism. Extrapolating from their lowest energy ($\sqrt{s} = 20$ GeV) for pPb, we have at $\sqrt{s} = 14$ GeV:

$$\sigma_{\mathrm{Tot}}^{p\mathrm{Pb}} \approx 2850\mathrm{mb}, \qquad \sigma_{\mathrm{El}}^{p\mathrm{Pb}} \approx 1050\mathrm{mb} \qquad \Rightarrow \sigma_{\mathrm{InEl}}^{p\mathrm{Pb}} \approx 1800\mathrm{mb} \tag{11}$$

In comparison, a simple $A^{2/3}$ scaling of the pp total cross section (Eq. 10) to pPb *inelastic* cross section yields 1350 mb. In any case, knowledge of the total inelastic cross section to within a factor of two is sufficient to gain a qualitative understanding of background of heavy projectiles.

Consider now the flux of ions produced by a 1 Amp beam of Pb nuclei at 110 GeV/u scattering from a residual gas of mostly H_2 molecules at 10^{-9} milliBar. In a 10 m segment of the beam pipe at ambient temperature there is an areal density of $\rho L \approx 5 \cdot 10^{10}$ H/cm^2. The total nuclear break-up rate per 10 m is

$$R_{\text{Residual Gas}} = [\rho L]\,\frac{I}{82e}\sigma_{\mathrm{InEl}} \approx 7000/\mathrm{sec} \tag{12}$$

The neutron background studies presented in Fig. 5 included all interactions of the proton beam from a range of up to 50 m upstream of the IP. However, actual backgrounds in the forward region were found to be dominated by beam-gas interactions in the nearest ~ 10 m. Heavy ion fragments produced from beam-gas interactions near the Roman Pot detectors will likely not leave the beam envelope. In contrast, protons and other light ion fragments (with rigidities very different from the beam particles) will likely not reach the detectors at the second focus, unless they are produced in the last 20 m before the detectors (13 m drift space after dipole ionBXDS01A plus the magnets ionBXDS01B and ionQDS01 of Table 1). Taking into consideration that each nuclear dissociation event would typically produce one light and one heavy fragment, we estimate a beam-gas induced background flux of:

$$\text{14000 events/ sec with an typical charged particle multiplicity of 2.} \tag{13}$$

Assuming the Roman Pot tracking detectors as well as this proposed mini-DIRC can resolve the ~ 8 ns bunch structure, this is a pile-up probability of $\approx 2 \cdot 10^{-4}$.

3.2 Photo-dissociation in eA Collisions

Ion beam loss effects from eA beam collisions were estimated by S. Klein [10]. We follow a similar approach. The total eA cross section is dominated by quasi-real photon production.

This can be expressed in an equivalent radiator (t^V) formalism as

$$\sigma_{eA} = \int_{\text{Threshold}}^{s} \frac{t^V(W^2, s)}{W^2 - M^2} \sigma_{\gamma A}(W^2) dW^2$$
$$t^V \approx \frac{\alpha}{\pi} \log\left[\frac{Q^2_{\text{Max}}}{Q^2_{\text{Min}}}\right] \left[1 - \frac{W^2 - M^2}{s - M^2} + \frac{1}{2}\left(\frac{W^2 - M^2}{s - M^2}\right)^2\right] \tag{14}$$

where $\sqrt{s}$ is the total eA CM energy, W is the total γA CM energy, and M is the projectile ion mass. In collider kinematics with incident and scattered electron energies k and k', respectively:

$$Q^2_{\text{Min}} = m_e^2 \frac{(|\mathbf{k}| - |\mathbf{k}'|)^2}{|\mathbf{k}|\,|\mathbf{k}'|} \tag{15}$$

Based on the elastic nuclear form factor, we take

$$Q^2_{\text{Max}} = \frac{3}{5}\left[\frac{2\hbar c}{r_0 A^{1/3}}\right]^2, \qquad \text{with } r_0 = 0.95 \text{ fm.} \qquad \text{For } ^{208}\text{Pb:} \quad Q^2_{\text{Max}} = 0.003 \text{ GeV}^2. \tag{16}$$

The resulting equivalent radiator spectrum is illustrated in Fig. 7. We estimate the integral of Eq. 14 in two components: The Giant Dipole Resonance (GDR) plus an incoherent γN continuum above pion threshold.

To simplify the estimate of incoherent photo-nuclear absorption above pion threshold, we constructed a Regge fit (Fig. 8) of the γp total cross sections using the Donnachie and Landshoff exponents of Eq. 10:

$$\sigma_{\gamma N}(W^2) = (69\mu b)\left[\frac{W^2 - M^2}{2M}\right]^{0.0808} + (115\mu b)\left[\frac{W^2 - M^2}{2M}\right]^{-0.4525} \tag{17}$$

The integral of this cross section, weighted by the equivalent radiator flux of quasi-real photons and multiplied by a luminosity of $10^4/(\mu\text{b sec})$ per nucleon is

$$\text{Rate}^{\text{Incoherent}}_{eA} = 6.8 \cdot 10^5/\text{sec.} \tag{18}$$

The low CM energy (W) contribution to the photo-nuclear cross section is dominated by the Giant Dipole Resonance (GDR). Berman and Fultz ([11] Fig. 41) gave a semi-analytic formula for the inverse energy weighted cross section in the ion rest frame:

$$\sigma_{-1} = \int \frac{d\omega}{\omega}\sigma(\omega) = \frac{4\pi\alpha}{3}\frac{NZ}{A-1}\langle r^2\rangle \approx \frac{4\pi\alpha}{3}\frac{NZA^{2/3}}{A-1}(0.95 \text{ fm})^2 \approx (180\,\mu\text{b})A^{4/3} \tag{19}$$

We assume the luminosity *per nucleus* scales as $1/A$ relative to the ep luminosity. With a peak design ep luminosity $\mathcal{L}_{ep} = 10^{34}/\text{cm}^2/\text{sec}$ at 10×275 GeV^2 ep collisions, we obtain:

$$\text{GDR Rate} = \frac{\mathcal{L}_{ep}}{A} t^V(x_{GDR})\sigma_{-1} = (10^4/\mu\text{b/sec})\,(0.077)\,(180\,\mu b)A^{1/3}$$
$$\approx 8 \cdot 10^5/\text{sec on } ^{208}\text{Pb} \tag{20}$$

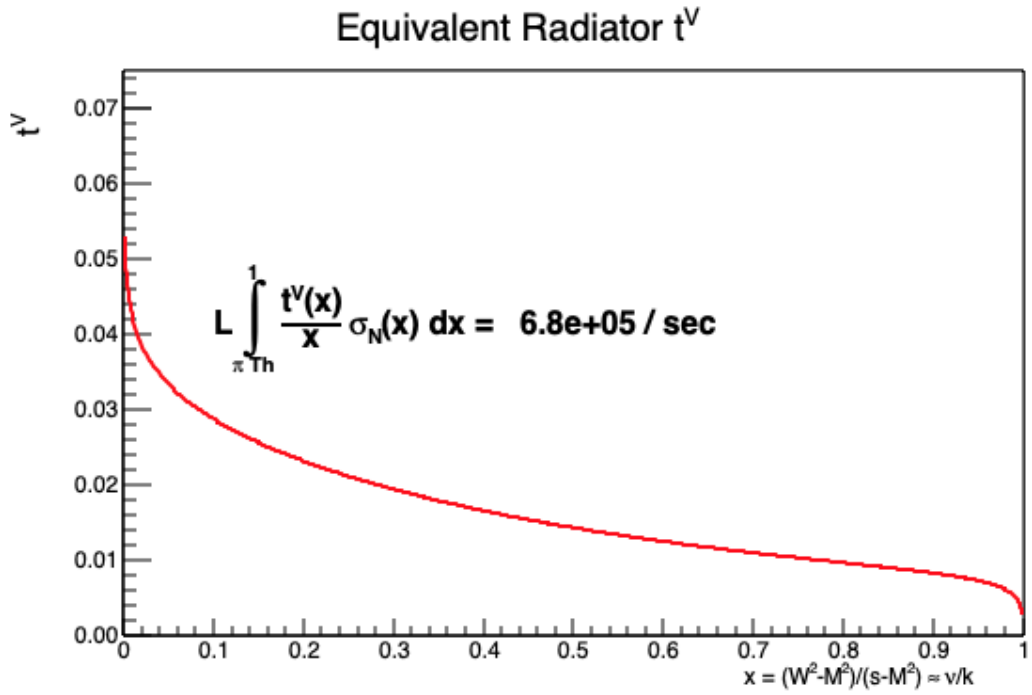

Figure 7: Equivalent radiator (Eq. 14) for eA collisions $10 \times 108A$ GeV^2. Note $\nu = k - k'$ in detector frame, not the invariant variable. The integrated incoherent rate is for ^{208}Pb or other similar heavy ion beam with luminosity per nucleon of $10^4/(\mu\text{b sec})$.

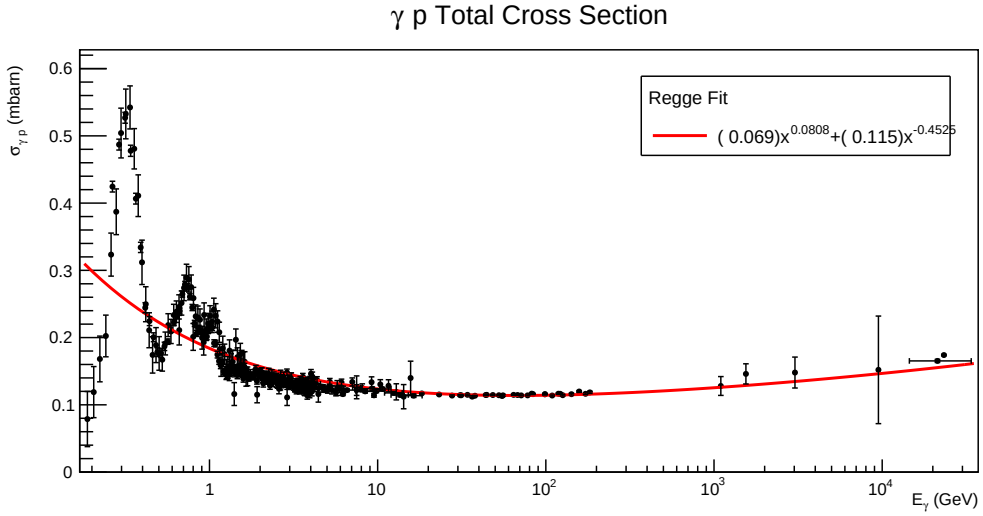

Figure 8: Simple Regge-inspired fit to γp total cross sections. Data tabulation from [3].

Combining Eqs. 18 and 20 we estimate a total eA rate $\approx 1.5 \cdot 10^5$/sec. We note that this rate from eA collisions is an order of magnitude higher than the estimate in Eq. 13 of beam-gas interactions. Given an 8 nsec beam crossing period, and assuming the Roman Pot trackers (e.g. AC-LGAD) and this Cherenkov detector can resolve the bunches, the resulting pile-up probability per bunch crossing is $\approx 0.12\%$. In two-detector operation, the two IPs will share the current, and the time between bunch collisions will double, resulting in exactly the same pile-up probability of random background contaminating a physics event. We note these background events could have high multiplicity (especially if one of the fragments produces a hadronic shower near the second focus detectors). This would effect the severity of the pile-up event, but does not change the overall probability of $\sim 0.1\%$ for a physics event to be contaminated by background pile-up.

4 Light Collection and Photo-Sensor Studies

We will use the GSI DIRC simulation code to evaluate various performance issues of the proposed detector. The starting geometry is as follows:

- A fused silica bar, 0.6 cm thick along the beam direction, 3 cm tall, and 15 cm wide perpendicular to the beam direction.
- An expansion volume 3 cm long, spreading the light out to a $3 \times 3\text{cm}^2$ photo-sensor surface.
- Various potential photo-sensors, including SiPMT/MPPC, MCP-PMT, and conventional PMT.

4.1 Year One Deliverables

The raw Poisson photo-statistics are more than sufficient to resolve *e.g.* $z = 90$ from $z = 90 \pm 1$ as well as protons from helium, and every element in between. However, there are many effects that could degrade the performance relative to pure Poisson statistics. The following potential effects will be the focus of simulation studies in the first year:

1. Variations in light collection for different impact points of the incident ion (Fig. 1).
2. Pulse height dependence on variations of light illumination of the photo-sensor surface. These studies will incorporate known typical efficiency and gain variations across the surface of existing SiPM and MCP-PMT photosensors.
3. Fluctuations in light yield from energetic δ-rays. These can be generated either inside the silica bar itself, or in upstream elements such as the Roman Pot window.
4. Photo sensor dynamic range and gain saturation simulation studies. From protons to U, we anticipate a dynamic range of $1 : 10^4$ in Cherenkov light yield. A non-linear gain *vs* amplitude does not, in and of itself, preclude $\Delta z \leq 1$ resolution, but it will

complicate calibrations. The known saturation properites of both SiPM and MCP-PMT photosensors will determine the minimum feasible size of the expansion volume and photosensor array. Note we are not imaging Cherenkov 'rings', but are measuring absolute light output.

5. Backgrounds from eA physics collisions at the IP and rescattered particles. Goal to compare primary eA processes from FLUKA and the fragmentation models of Fig. 1 (B.Moran [1]). These studies will use the IR8 optics simulation developed for the studies illustrated in Fig. 1, and will focus on charged particle tracks in the SiO_2 radiator.

4.2 Quartz Manufacturing Quality Control

The generation and detection of Cherenkov photons is a key aspect of the success of the proposed detector. The optimized detector performance is based on the assumption of quartz material with quality that is equivalent to the BaBar DIRC. However, a few recent R&D efforts demonstrated that sourcing high-quality quartz material can be a challenge.

SBU holds 5 bars of 15 cm x 1 cm x 0.5 cm quartz fingers (from past R&D effort) with high manufacturing quality similar to the BaBar DIRC quartz. These will be part of the in-kind contribution from SBU to the Mini-DIRC project, and could potentially be used in a prototype. Furthermore, SBU will continue pursuing the new vendors for high-quality quartz and perform tests to verify the claimed specifications.

5 Prototype and Beam Tests

5.1 Year 2

Depending upon the simulation studies described above, we will request funding in year 2 as follows.

- Procurement of one or more sample photosensors and tests of dynamic range, gain saturation, and noise with a variable light source.
- Procurement of a fused silica radiator bar, light guide, and enclosure to construct a prototype for beam tests.

5.2 Year 3

Beam tests. Potential options include electrons in the test facility of the Jefferson Lab Hall D Pair Spectrometer, FermiLab proton and hadron beams, CERN test beams.

6 Equity

6.1 Cost Effectiveness

This proposal includes extensive "in-kind" contributions of expertise. We have negotiated a low off-campus indirect cost rate from the Old Dominion University Research Foundation of 26% of direct costs (no IDC is charged to tuition).

6.2 Diversity, Equity, and Inclusion

All of the signatories are committed to providing a work environment that supports all participants and actively recruit members of underrepresented groups. Old Dominion University is a Carnegie R-1 institution, with over 50% enrollment of racial/ethnic minority students [12]. A recent global survey ranked ODU as 4th in the U.S. in the category of "Reduced Inequalities"[13]. In the experimental nuclear physics group at Old Dominion University, four of eight graduate students are women. Recent graduates from the group include Torri Jesske, currently a Post-Doc at JLab and Holly Szumila-Vance, currently a Staff Scientist at JLab.

6.3 Post-Doc and Graduate Student Support and Mentoring and Support

The ODU Experimental Research Group will provide funding, as necessary, to sustain the Post Doc and Graduate Student at 100% FTE. This will entail proportional effort on other projects and includes support if this project is not extended beyond Year 1. The direct supervisor of the Post-Doc and/or graduate student will be Prof. C. Hyde (ODU). The travel budget is essential to the project, and will also ensure the Post-Doc and Graduate student receive mentoring that reflects the expertise of the full collaboration.

7 Year One Budget

Project period 1 Oct 2023 – 30 Sep 2024. Budget detail for full funding of year one is listed in Table 2. Summary of budgets at 100%, 80%, or 60% are listed in Table 3.

1. Full Funding: 100%. Total budget $\$117,000$.

   - 50% FTE Post Doc (ODU)
   - 100% FTE Graduate Student (ODU)
   - Foreign travel: one visit either from ODU to GSI, or GSI to ODU/JLab for training/collaborating on GSI DIRC simulation software.
   - Domestic travel: Graduate student or Post Doc travel from ODU to SBU for consultations on photo-sensor properties and dynamic range effects.

2. 80% Funding.Total budget $\$92,000$.

   - 50% FTE Post Doc (ODU)
   - 50% FTE Graduate Student (ODU)
   - Adjusted travel

   Deliverable (section 4.1)# 4: Photo sensor saturation studies will be limited in scope: *e.g.* semi-analytic analysis.
   Deliverable (section 4.1)# 5: Background simulations will include only one eA model.

3. 60% Funding. Total budget: $\$69,000$

   - 50% FTE Post Doc (ODU)
   - Travel expanded to allow compensating face-to-face interactions of Post Doc, P.I.s and collaborators. SBU.

   Photo sensor studies would focus on Deliverable (section 4.1)# 1. Background studies would be further curtailed.

Institutional Responsibilities (Year 1)

GSI: Provide DIRC simulation code and usage training and guidance.

ODU: Cherenkov light collection simulations. Photo sensor response simulations

SBU: Advice and guidance on challenges and solutions of photo-sensor response to pulses with event-by-event dynamic range up to 10,000:1 ($z = 90 : 1$). Quantify the requirement for manufacturing the quartz bars. Assistance with implementation of IR8 optics.

Table 2: Budget Detail: ODU (Full Funding)

Item	Description	Salary	Fringe	Subtotal
1	PostDoc (50% FTE)	$31,000	$16,000	$47,000
2	Graduate Student (100% FTE)	$30,000	$ 2,235	$32,235
3	Foreign Travel			$ 4,000
4	Domestic Travel			$ 2,117
5	Subtotal (Items 1–4)			$85,352
6	IDC: 26% of Item 4 (Off-Campus rate)			$22,192
7	Tuition (IDC exempt)			$ 9,456
8	**Total** (Items 5,6,7)			**$117,000**

Table 3: Budget Summaries (ODU)

Budget: 100%			
Item	Description	Subtotal Direct	Total with IDC
1	ODU Post Doc (50% FTE)	$47,000	$59,220
2	ODU Grad Student (100% FTE)	$41,691	$50,072
3	Travel	$6,117	$7,708
	Total 100% Budget		**$117,000**
Budget: 80%			
1	ODU Post Doc (50% FTE)	$47,000	$59,220
2	ODU Grad Student (50% FTE)	$20,846	$25,036
3	Travel	$6,146	$7,744
	Total 80% Budget		**$92,000**
Budget: 60%			
1	ODU Post Doc (50% FTE)	$47,000	$59,220
2	Travel	$7,762	$9,780
	Total 60% Budget		**$69,000**

References

[1] B. Moran, B. Schmookler, et al. Study of exotic nuclei made easy – a potentially novel topic for physics at the EIC, 2022. Contribution to DIS2022.

[2] EIC Detector Proposal Advisory Panel report . `https://www.bnl.gov/dpapanelmeeting/files/pdf/dpap_report_3-21-2022_final.pdf`, 2022.

[3] R. L. Workman et al. Review of Particle Physics. *Prog. Theor. Exp. Phys.*, 2022:083C01, 2022.

[4] Mikhail N. Polyanskiy. Refractive index database. https://refractiveindex.info. Accessed on 2022-07-06.

[5] Hamamatsu MCP-PMT R10754-07-M16
. Accessed on 2022-07-08.

[6] C. Hyde et al. eRD21: EIC Background Studies and the Impact on the IR and Detector. https://wiki.bnl.gov/conferences/index.php?title=March_2021, 2021.

[7] R. Gamage et al. IR8 Status. https://indico.bnl.gov/event/18414/contributions/76160/, May 17-19, 2023.

[8] A. Donnachie and P. V. Landshoff. Total cross-sections. *Phys. Lett. B*, 296:227–232, 1992.

[9] V. Guzey and M. Strikman. Proton-nucleus scattering and cross section fluctuations at RHIC and LHC. *Phys. Lett. B*, 633:245–252, 2006.

[10] Spencer R. Klein. Heavy ion beam loss mechanisms at an electron-ion collider. *Phys. Rev. ST Accel. Beams*, 17(12):121003, 2014.

[11] B. L. Berman and S. C. Fultz. Measurements of the giant dipole resonance with monoenergetic photons. *Rev. Mod. Phys.*, 47:713–761, 1975.

[12] ODU Ranked Among Top 15% of US Colleges and Universities for Diversity. https://www.odu.edu/article/odu-ranked-among-the-top-15-of-us-colleges-and-universities-for-diversity, 2021.

[13] Times Higher Education Rankings. https://www.timeshighereducation.com/impactrankings, 2023.